

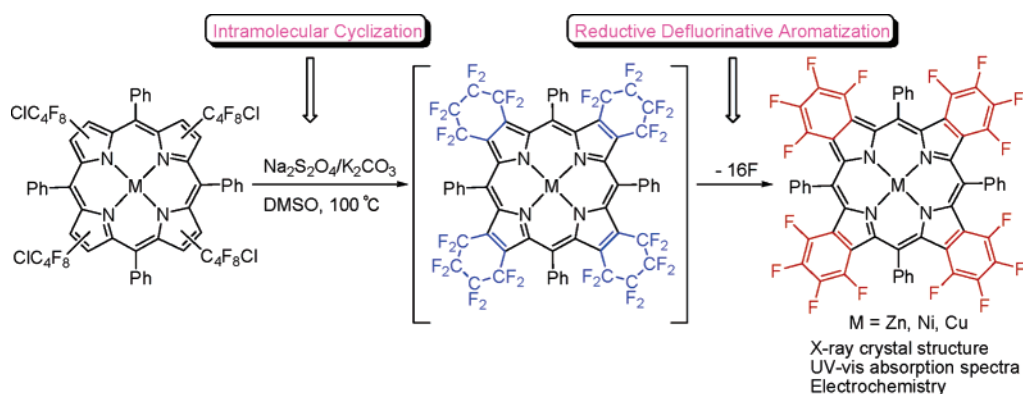
C–F Bond Activation by Modified Sulfinatodehalogenation: Facile Synthesis and Properties of Novel Tetrafluorobenzoporphyrins by Direct Intramolecular Cyclization and Reductive Defluorinative Aromatization of Readily Available β -Perfluoroalkylated Porphyrins

Chao Liu,[†] Dong-Mei Shen,[†] Zhuo Zeng,[‡] Can-Cheng Guo,^{*,§} and Qing-Yun Chen^{*,†,§}

Key Laboratory of Organofluorine Chemistry, Shanghai Institute of Organic Chemistry, Chinese Academy of Sciences, 354 Fenglin Road, Shanghai 200032, China, College of Chemistry and Environment, South China Normal University, Guangzhou 510631, China, and College of Chemistry and Chemical Engineering, Hunan University, Changsha 410082, China

chenqy@mail.sioc.ac.cn

Received August 23, 2006



A facile and efficient synthesis of various novel fluorinated extended porphyrins has been developed. The method is based on the direct intramolecular cyclization and reductive defluorinative aromatization of readily available β -perfluoroalkylated porphyrins by highly selective C–F bond activation under modified sulfinatodehalogenation reaction conditions. Various β -(ω -chloroperfluoroalkyl)-*meso*-tetraphenylporphyrins prepared readily by sulfinatodehalogenation reaction or palladium-catalyzed cross-coupling reaction were treated with $\text{Na}_2\text{S}_2\text{O}_4/\text{K}_2\text{CO}_3$ (10:10 equiv per R_F tail) in DMSO at 100 °C for 10–30 min, resulting in good yields of novel β -tetrafluorobenzo-*meso*-tetraphenylporphyrins. That further reduction of C–F bonds of the products was not observed under the optimal conditions indicates the high selectivity of the reaction. It was found that the amount of sodium dithionite, base, and central metal ion of substrate porphyrins play important roles in the reaction. Detailed mechanism investigations and systematic studies on X-ray crystallographic structure and photophysical and electrochemical properties of a series of new tetrafluorobenzoporphyrins are also reported.

Introduction

Activation and functionalization of C–F bonds provides a chemical challenge akin to that of C–H activation in analogous hydrocarbon compounds because fluorocarbons are noted for their chemical inertness, which is a manifestation of the great strength of the C–F bond. Although these same thermodynamic

and kinetic considerations tend to disfavor C–F bond activation, numerous examples of defluorination of saturated fluorocarbons have been reported in the past decade.^{1–5} However, selective reduction of perfluoroalkanes is always a challenge analogous to that of achieving alkane functionalization by selective oxidation chemistry. Recently, the use of organometallic

[†] Shanghai Institute of Organic Chemistry.

[‡] South China Normal University.

[§] Hunan University.

(1) For comprehensive reviews on C–F bond activation, see the following: (a) Richmond, T. G. *Angew. Chem., Int. Ed.* **2000**, *39*, 3241–3244. (b) Saunders, G. C. *Angew. Chem., Int. Ed.* **1996**, *35*, 2615–2617. (c) Kiplinger, J. L.; Richmond, T. G. *Chem. Rev.* **1994**, *94*, 373–431.

complexes offers a versatile and powerful means with which to activate C–F bonds selectively.^{1–5} For example, Crabtree and co-workers have made significant contributions in developing reagents and photosensitization techniques to defluorinate perfluoroalkanes using transition-metal-containing organometallic reagents.³ Richmond's group has shown that the defluorination chemistry can be achieved utilizing early transition metallocenes and amalgamated aluminum or magnesium as the final reductant.⁴ Hughes and co-workers have illustrated simple hydrogenation of a perfluorocarbon under mild conditions using various organometallic complexes.⁵ However, they generally use reagents that are inconvenient and expensive. During our ongoing efforts in the synthesis and application of perfluoroalkylated porphyrins,⁶ we have found unexpectedly a convenient and inexpensive intramolecular cyclization and reductive defluorinative aromatization method for the synthesis of novel fluorinated extended porphyrins directly from readily available β -perfluoroalkylated porphyrins by highly selective C–F bond activation based on a modified sulfinatodehalogenation reaction.^{6d}

It is well-known that porphyrins form an important class of chromophores that are being developed and used for many different applications such as photodynamic therapy (PDT),

applications in the commercial dye industry, nonlinear absorption, artificial photosynthesis, oxygen transport, and solar energy conversion.⁷ Much research has been done to develop new porphyrin chromophores that display certain characteristics dependent on the application. Beginning with singlet oxygen sensitization and tumor therapy (PDT),⁸ the near-infrared-absorbing porphyrinoids have wide application in many scientific fields, such as biomedical imaging and the development of nonlinear optical materials.⁷ So far, there are mainly three ways to shift the absorption bands of porphyrinoids into the lower energy region, which include expanding the basic tetrapyrrolic macrocycle by adding extra pyrrolic fragments,⁹ increasing the macrocycle nonplanar deformation by introducing peripheral substituents,¹⁰ and extending the porphyrin core by fusing it with external aromatic fragments.¹¹ The latter approach forms a class of so-called " π -extended porphyrins", which possess interesting properties, inviting applications in various branches of optical technology and biomedicine. For example, tetrabenzoporphyrins have been found to be useful in PDT and biological oxygen imaging and have shown potential in optical limiting.¹² However, compared to regular porphyrins, the chemistry of benzoporphyrins has been little explored, mainly because of their limited synthetic availability.

In the past several years considerable progress has been made in the synthesis of *meso*-tetraarylated extended porphyrins, and some studies of their photophysical properties have been conducted. However, only a few experimental studies address the effects of nonplanarity in π -conjugated porphyrins, which can also be ascribed to their limited synthetic availability. Studies on the synthesis and properties of these molecules constitute the main focus of the present work. The extension of porphyrin pyrrole by fused benzene fragments can be achieved by three major methods: (1) a template condensation method;^{9b} (2) a retro-Diels-Alder method;¹³ or (3) an oxidative aromati-

(2) For recent and selective reports on C–F bond activation, see the following: (a) Paul, A.; Wannere, C. S.; Kasalova, V. *J. Am. Chem. Soc.* **2005**, *127*, 15457–15469. (b) Garratt, S. A.; Hughes, R. P.; Kovacic, I.; Ward, A. J.; Willemsen, S.; Zhang, D. *J. Am. Chem. Soc.* **2005**, *127*, 15585–15594. (c) Hughes, R. P.; Laritchev, R. B.; Zakharov, L. N.; Rheingold, A. L. *J. Am. Chem. Soc.* **2005**, *127*, 6325–6334. (d) Hughes, R. P.; Laritchev, R. B.; Zakharov, L. N.; Rheingold, A. L. *J. Am. Chem. Soc.* **2004**, *126*, 2308–2309. (e) Reinhold, M.; McGrady, J. E.; Perutz, R. N. *J. Am. Chem. Soc.* **2004**, *126*, 5268–5276. (f) Bardin, V. V.; Trukhin, D. V.; Adonin, N. Y.; Sxarichenko, V. F. *J. Fluorine Chem.* **2004**, *125* (10), 1431–1435. (g) Yang, Z. Y. *J. Org. Chem.* **2004**, *69*, 2394–2403. (h) Terao, J.; Ikumi, A.; Kuniyasu, H.; Kambe, N. *J. Am. Chem. Soc.* **2003**, *125*, 5646–5647. (i) Noveski, D.; Braun, T.; Schuller, M.; Neumann, B.; Stammler, H. G. *Dalton Trans.* **2003**, *21*, 4075–4083. (j) Kuhl, S.; Schneider, R.; Fort, Y. *Adv. Synth. Catal.* **2003**, *345* (3), 341–344. (k) Kraft, B. M.; Jones, W. D. *J. Organomet. Chem.* **2002**, *658* (1–2), 132–140. (l) Guennou De Cadenet, K.; Rumin, R.; Petillon, F. Y.; Yufit, D. S.; Muir, K. W. *Eur. J. Inorg. Chem.* **2002**, *3*, 639–657. (m) Kirkham, M. S.; Mahon, M. F.; Whittlesey, M. K. *Chem. Commun.* **2001**, *9*, 813–814. (n) Bohm, V. P. W.; Gstottmayr, C. W. K.; Weskamp, T.; Herrmann, W. A. *Angew. Chem., Int. Ed.* **2001**, *40*, 3387–3388. (o) Ricciardi, G.; Belviso, S.; Lelj, F. *Inorg. Chem.* **2000**, *39*, 1618–1620.

(3) (a) Burdeniuc, J.; Chupka, W.; Crabtree, R. H. *J. Am. Chem. Soc.* **1995**, *117*, 10119–10120. (b) Burdeniuc, J.; Crabtree, R. H. *J. Am. Chem. Soc.* **1996**, *118*, 2525–2526. (c) Burdeniuc, J.; Crabtree, R. H. *Science* **1996**, *271*, 340–341.

(4) (a) Kiplinger, J. L.; Richmond, T. G. *J. Am. Chem. Soc.* **1996**, *118*, 1805–1806. (b) Beck, C. M.; Park, Y. J.; Crabtree, R. H. *Chem. Commun.* **1996**, 1115–1116. (c) Bennett, B. K.; Harrison, R. G.; Richmond, T. G. *J. Am. Chem. Soc.* **1994**, *116*, 11165–11166. (d) Harrison, R. G.; Richmond, T. G. *J. Am. Chem. Soc.* **1993**, *115*, 5303–5304.

(5) (a) Hughes, R. P.; Husebo, T. L.; Maddock, S. M.; Rheingold, A. L.; Guzei, I. A. *J. Am. Chem. Soc.* **1997**, *119*, 10231–10232. (b) Hughes, R. P.; Linder, D. C.; Rheingold, A. L.; Liable-Sands, L. M. *J. Am. Chem. Soc.* **1997**, *119*, 11544–11545. (c) Hughes, R. P.; Smith, J. M. *J. Am. Chem. Soc.* **1999**, *121*, 6084–6085.

(6) (a) Liu, C.; Shen, D. M.; Chen, Q. Y. *Chem. Commun.* **2006**, 770–772. (b) Liu, C.; Shen, D. M.; Chen, Q. Y. *Eur. J. Org. Chem.* **2006**, 2703–2706. (c) Liu, C.; Chen, Q. Y. *Eur. J. Org. Chem.* **2005**, 3680–3686. (d) Zeng, Z.; Liu, C.; Jin, L. M.; Guo, C. C.; Chen, Q. Y. *Eur. J. Org. Chem.* **2005**, 306–316. (e) Shen, D. M.; Liu, C.; Chen, Q. Y. *Chem. Commun.* **2005**, 4982–4984. (f) Liu, C.; Chen, Q. Y. *Synlett* **2005**, *8*, 1306–1310. (g) Zeng, Z.; Jin, L. M.; Guo, C. C.; Chen, Q. Y. *Acta Chim. Sin.* **2004**, *62*, 288–294. (h) Chen, L.; Jin, L. M.; Guo, C. C.; Chen, Q. Y. *Synlett* **2005**, *6*, 963–970. (i) Jin, L. M.; Chen, L.; Guo, C. C.; Chen, Q. Y. *J. Porphyrins Phthalocyanines* **2005**, *9*, 109–120. (j) Jin, L. M.; Chen, L.; Yin, J. J.; Guo, C. C.; Chen, Q. Y. *J. Fluorine Chem.* **2005**, *126*, 1321–1326. (k) Jin, L. M.; Zeng, Z.; Guo, C. C.; Chen, Q. Y. *J. Org. Chem.* **2003**, *68*, 3912–3917. (l) Jin, L. M.; Chen, L.; Yin, J. J.; Zhou, J. M.; Guo, C. C.; Chen, Q. Y. *J. Org. Chem.* **2006**, *71*, 527–536. (m) Shen, D. M.; Liu, C.; Chen, Q. Y. *J. Org. Chem.* **2006**, *71*, 6508–6511.

(7) *The Porphyrin Handbook*; Kadish, K. M., Smith, K. M., Guillard, R., Eds.; Academic Press: San Diego, CA, 2000–2003; Vols. 1–20.

(8) (a) Nyman, E. S.; Hynninen, P. H. *J. Photochem. Photobiol. B* **2004**, *73*, 1–2. (b) Moan, J.; Peng, Q. *Anticancer Res.* **2003**, *23*, 3591–3600. (c) Brunner, H.; Schellerer, K. M. *Monatsh. Chem.* **2002**, *133*, 679–705. (d) Pandey R. K. In *The Porphyrin Handbook*; Kadish, K. M., Smith, K. M., Guillard, R., Eds.; Academic Press: San Diego, CA, 2000; Vol. 6, Chapter 43.

(9) (a) Sessler, J. L.; Seidel, D. *Angew. Chem., Int. Ed.* **2003**, *42*, 5134–5175. (b) Sessler, J. L.; Gebauer, A.; Vogel E. In *The Porphyrin Handbook*; Kadish, K. M., Smith, K. M., Guillard, R., Eds.; Academic Press: San Diego, CA, 2000; Vol. 2, Chapter 9.

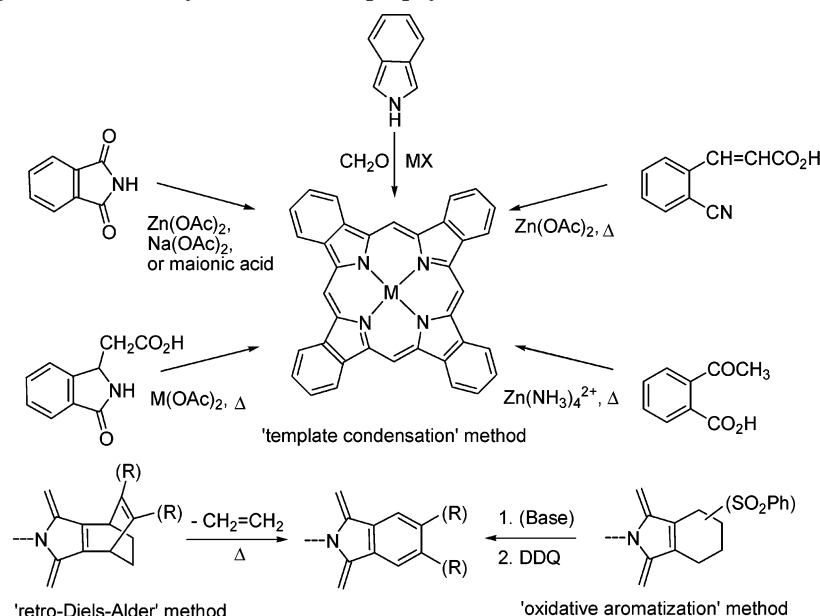
(10) (a) Senge, M. O. *Chem. Commun.* **2006**, 243–256. (b) Senge M. O. In *The Porphyrin Handbook*; Kadish, K. M., Smith, K. M., Guillard, R., Eds.; Academic Press: San Diego, CA, 2000; Vol. 1, Chapter 6.

(11) (a) Lash, T. D. *J. Porphyrins Phthalocyanines* **2001**, *5*, 267–288. (b) Lash T. D. In *The Porphyrin Handbook*; Kadish, K. M., Smith, K. M., Guillard, R., Eds.; Academic Press: San Diego, CA, 2000; Vol. 2, Chapter 10.

(12) For recent and selective reports, see the following: (a) Rietveld, I. B.; Kim, E.; Vinogradov, S. A.; *Tetrahedron* **2003**, *59*, 3821–3831. (b) Souid, A. K.; Tacka, K. A.; Galvan, K. A.; Penefsky, H. S. *Biochem. Pharm.* **2003**, *66*, 977–987. (c) Friedberg, J. S.; Skema, C.; Baum, E. D.; Burdick, J.; Vinogradov, S. A.; Wilson, D. F.; Horan, A. D.; Nachamkin, I. J. *J. Antimicrob. Chemother.* **2001**, *48*, 105–107. (d) Ono, N.; Ito, S.; Wu, C. H.; Chen, C. H.; Wen, T. C. *Chem. Phys.* **2000**, *262*, 467–473. (e) Brunel, M.; Chaput, F.; Vinogradov, S. A.; Campagne, B.; Canva, M.; Boilot, J. P. *Chem. Phys.* **1997**, *218*, 301–307.

(13) (a) Ito, S.; Murashima, T.; Uno, H.; Ono, N. *Chem. Commun.* **1998**, 1661–1662. (b) Ito, S.; Ochi, N.; Murashima, T.; Uno, H.; Ono, N. *Heterocycles* **2000**, *52*, 399–411. (c) Ito, S.; Uno, H.; Murashima, T.; Ono, N. *Tetrahedron Lett.* **2001**, *42*, 45–47. (d) Uno, H.; Ishikawa, T.; Hoshi, T.; Ono, N. *Tetrahedron Lett.* **2003**, *44*, 5163–5165. (e) Shimizu, Y.; Shen, Z.; Okujima, T.; Uno, H.; Ono, N. *Chem. Commun.* **2004**, 374–375. (f) Yamada, H.; Kushibe, K.; Okujima, T.; Uno, H.; Ono, N. *Chem. Commun.* **2006**, 383–385.

SCHEME 1. Three Major Methods for Synthesis of Benzoporphyrins



zation method¹⁴ (Scheme 1). However, the first method is quite impractical, suffering from low yields and a large number of side products because of the extremely harsh conditions required for the macrocycle assembly (i.e., fusion at 350–400 °C). Although the latter two methods make it possible to obtain tetrabenzoporphyrins in high purity and acceptable yields, an obvious drawback is that they involve a multistep sequence.

In this paper, we present a more detailed account of the novel and appealing strategy for the synthesis of various novel tetrafluorobenzoporphyrins, which is based on the direct intramolecular cyclization and reductive defluorinative aromatization of readily available β -perfluoroalkylated porphyrins by highly selective C–F bond activation under modified sulfinate dehalogenation reaction conditions. In addition, we report the systematic X-ray crystallographic structure and photophysical and electrochemical properties of a series of novel tetrafluorobenzoporphyrins, indicating the considerable influence of fluorine atoms.

Results and Discussion

Synthesis of Various β -(ω -Chloroperfluoroalkyl)-*meso*-tetraphenylporphyrins. For the synthesis of β -mono(ω -chloroperfluoroalkyl)-*meso*-tetraphenylporphyrins, it was found that the sulfinate dehalogenation method was the most convenient and suitable one,^{6k} although there was another method available,^{6f} i.e., treatment of *meso*-tetraphenylporphyrin H₂TPP (**H₂1**) with perfluoroalkyl iodides R_FI (**2**) in the presence of Na₂S₂O₄ and NaHCO₃ in a solvent mixture of DMSO/CH₂Cl₂ (1:1 v/v) at 30–40 °C for several hours, that directly resulted in the corresponding β -mono(ω -chloroperfluoroalkyl)-*meso*-tetraphenylporphyrins in acceptable yields. However, a larger excess of R_FI (50 equiv) had to be used to ensure smooth reaction. This drawback prompted us to further investigation on the reaction condition, which revealed that a smaller amount of R_FI (10 equiv) could also enable us to obtain the desired β -mono(ω -chloroperfluoroalkyl)-*meso*-tetraphenylporphyrins in comparable yields if higher temperature and relatively longer reaction time were employed (Scheme 2).

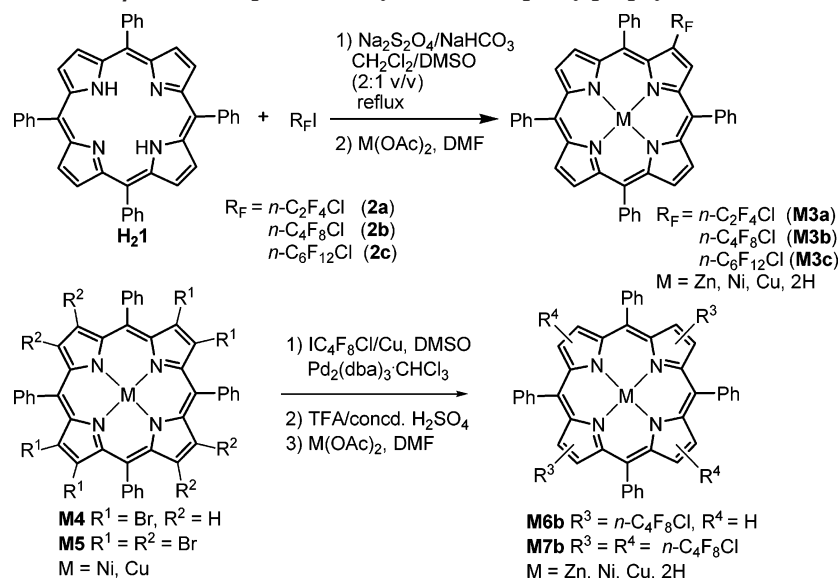
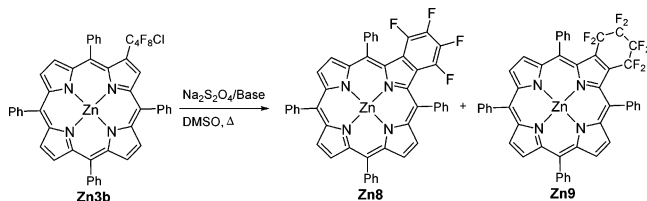
β -Di- and β -tetra(ω -chloroperfluoroalkyl)-*meso*-tetraphenylporphyrins were conveniently prepared by the palladium-

catalyzed cross-coupling reaction of readily available bromoporphyrins with R_FI/Cu in DMSO according to our recent report^{6f} (Scheme 2). It is worth mentioning that the reaction proceeded smoothly and resulted in similar yields of the desired products in the absence of the poisonous AsPh₃ ligand.

Intramolecular Cyclization and Reductive Defluorinative Aromatization of Various β -(ω -Chloroperfluoroalkyl)-*meso*-tetraphenylporphyrins. With various β -(ω -chloroperfluoroalkyl)-*meso*-tetraphenylporphyrins in hand, we initially investigated the reaction conditions in detail for the intramolecular cyclization and reductive defluorinative aromatization reaction with [β -mono(ω -chloroperfluorobutyl)-*meso*-tetraphenylporphyrinato]zinc (**Zn3b**) as model substrate. As illustrated in Table 1, on using the typical conditions of activation of the C–Cl bond of perfluoroalkyl chlorides in the modified sulfinate dehalogenation system (**Zn3b**/Na₂S₂O₄/NaHCO₃ = 1:1.5:1.5, in DMSO at 100 °C),¹⁵ the reaction only resulted in 59% conversion of the starting material and 1.8:1 ratio of [β -monotetrafluorobenzo-*meso*-tetraphenylporphyrinato]zinc (**Zn8**) to [β -mono(octafluorocyclohexenyl)-*meso*-tetraphenylporphyrinato]zinc (**Zn9**) (Table 1, entry 1). Increase in the ratio of **Zn8** to **Zn9** was achieved by elevated amounts of Na₂S₂O₄/NaHCO₃ (Table 1, entries 2 and 3). However, too much Na₂S₂O₄/NaHCO₃ may be harmful. When 50 equiv of Na₂S₂O₄/NaHCO₃ was employed, the reaction resulted in the formation of a significant

(14) (a) Finikova, O. S.; Galkin, A. S.; Rozhkov, V. V.; Cordero, M. C.; Hagerhall, C.; Vinogradov, S. A. *J. Am. Chem. Soc.* **2003**, *125*, 4882–4893. (b) Finikova, O. S.; Cheprakov, A.; Beletskaya, I.; Vinogradov, S. A. *Chem. Commun.* **2001**, 261–267. (c) Finikova, O. S.; Cheprakov, A. V.; Beletskaya, I. P.; Carroll, P. J.; Vinogradov, S. A. *J. Org. Chem.* **2004**, *69*, 522–535. (d) Finikova, O. S.; Cheprakov, A. V.; Carroll, P. J.; Vinogradov, S. A. *J. Org. Chem.* **2003**, *68*, 7517–7520. (e) Finikova, O. S.; Cheprakov, A. V.; Vinogradov, S. A. *J. Org. Chem.* **2005**, *70*, 9562–9572. (f) Ono, N.; Hideo, H.; Ono, K.; Kaneko, S.; Murashima, T.; Ueda, T.; Tsukamura, C.; Ogawa, T. *J. Chem. Soc., Perkin. Trans. 1* **1996**, 417–423. (g) Lash, T. D.; Roper, T. J. *Tetrahedron Lett.* **1994**, *35*, 7715–7718. (h) Lash, T. D.; Denny, C. P. *Tetrahedron* **1995**, *51*, 59–66. (i) Tome, A. C.; Lacerda, P. S. S.; Neves, M. G. P. M. S.; Cavaleiro, J. A. S. *Chem. Commun.* **1997**, 1199–1200. (j) Nguyen, L. T.; Senge, O. M.; Smith, K. M. *J. Org. Chem.* **1996**, *61*, 998–1003. (k) Vicente, M. G. H.; Tome, A. C.; Walter, A.; Cavaleiro, J. A. S. *Tetrahedron Lett.* **1997**, *38*, 3639–3642. (l) Jiao, L.; Hao, E.; Fronczek, F. R.; Vicente, M. G. H.; Smith, K. M. *Chem. Commun.* **2006**, 3900–3902.

(15) Long, Z. Y.; Chen, Q. Y. *J. Org. Chem.* **1999**, *64*, 4775–4728.

SCHEME 2. Synthesis of Various β -(ω -Chloroperfluoroalkyl)-*meso*-tetraphenylporphyrinsTABLE 1. Intramolecular Cyclization Aromatization of Zn3b under Various Conditions^a

entry	Na ₂ S ₂ O ₄ (equiv)	base (equiv)	T (°C)	t (min)	conv (%) ^b	Zn8/Zn9 ^b
1	1.5	NaHCO ₃ (1.5)	100	30	59	1.8
2	5	NaHCO ₃ (5)	100	30	100	7.6
3	10	NaHCO ₃ (10)	100	30	100	24.2
4	50	NaHCO ₃ (50)	100	30	100	21.5 ^c
5 ^d	10	NaHCO ₃ (10)	100	30	100	22.2 ^c
6	10	K ₂ CO ₃ (10)	100	30	100	42.9
7	10	K ₂ CO ₃ (10)	100	10	100	12.7
8	10	KOH (10)	100	30	100	<i>e</i>
9	10	NaH (10)	100	30	100	<i>e</i>
10	10	K ₂ CO ₃ (10)	70	30	100	6.5
11	10	K ₂ CO ₃ (10)	25	30	0	0
12	10	<i>f</i>	100	30	100	20.2

^a Reactions were carried out in DMSO (4 mL) under N₂ with Zn3b (20 mg, 1.0 equiv). ^b Determined by ¹⁹F NMR. ^c A significant amount of polar side product porphyrin sulfinate salt was formed. ^d Reaction was carried out in 4 mL of DMSO/H₂O (20:1 v/v). ^e Reaction only resulted in formation of Zn8 and no formation of Zn9 was observed, but partial degradation of the product was observed. ^f No base was used.

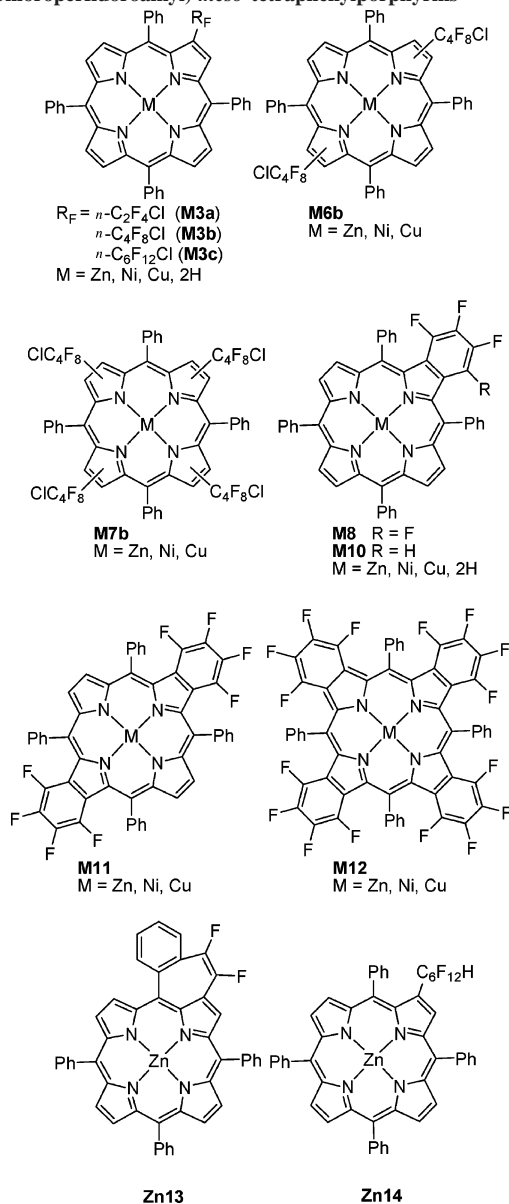
amount of polar side product, which was considered as the porphyrin sulfinate salt,¹⁵ although the conversion of Zn3b and ratio of Zn8 to Zn9 were essentially retained (Table 1, entry 4). This might be ascribed to any amount of H₂O produced from the decomposition of NaHCO₃ at higher temperature (100 °C) in the reaction.^{15,16} Indeed, a significant amount of the polar side product porphyrin sulfinate salt was also produced when 5% (v/v) H₂O was used as a cosolvent in DMSO (Table 1, entry 5). When K₂CO₃ was used as the base, the ratio of Zn8 to Zn9

increased to 42.9:1 (Table 1, entry 6). In the case of stronger bases KOH and NaH, side products and partial degradation of the desired products were observed, although no Zn9 was detected (Table 1, entries 8 and 9). In the absence of base, the reaction also proceeded smoothly and led to results similar to those for entry 3 (Table 1, entry 12). Elevated reaction temperatures facilitated the formation of Zn8; the ratio of Zn8 to Zn9 was only 6.5:1 when the reaction was carried out at 70 °C, whereas no formation of Zn8b and Zn9 was observed at 25 °C (Table 1, entries 10 and 11). All of these results suggested that a combination of 10 equiv of Na₂S₂O₄/K₂CO₃ in DMSO at 100 °C was the most effective system for the reaction. It should be pointed out that further reduction of C–F bonds of the aromatization product Zn8 was never observed even after a longer reaction time (4 h) under the optimal conditions, indicating the high selectivity of the reaction.

Under the optimal conditions, various β -(ω -chloroperfluoroalkyl)-*meso*-tetraphenylporphyrins were effectively subjected to the intramolecular cyclization and reductive defluorinative aromatization reaction to provide novel fluorinated extended porphyrins. As summarized in Table 2, the central metal ion of the substrate porphyrins played an important role in the reaction. For example, the Zn(II) complex Zn3b was effectively subjected to the reaction, providing the desired product Zn8 in excellent yield (Table 2, entry 1), whereas the reactions utilizing Ni(II) or Cu(II) porphyrin as a substrate gave relatively lower yields of the desired products (Table 2, entries 2 and 3). When the corresponding free base porphyrin H23b was used, the reaction resulted in 15% yield of intramolecular cyclization product H29 in addition to 60% yield of the desired product H28 (Table 2, entry 4). As expected, the reaction of β -di- and β -tetra(ω -chloroperfluorobutyl)-*meso*-tetraphenylporphyrins led to the corresponding new β -di- and β -tetra(tetrafluorobenzo)-*meso*-tetraphenylporphyrins in good yields (Table 2, entries 5–10). However, the latter turned out to be much less efficient than the former. The maximal yield achieved in the case of the latter was only 40% (Table 2, entry 8). The lower efficiency is likely to be caused by relatively poor stability of the resulting M12

(16) (a) Huang, W. Y. *J. Fluorine Chem.* **1992**, *58*, 1–8. (b) Huang, W. Y. *Isr. J. Chem.* **1994**, *39*, 167–170. (c) *Organofluorine Chemistry in China*; Huang, W. Y., Ed; Shanghai Science and Technology Press: Shanghai, 1996.

TABLE 2. Intramolecular Cyclization and Reductive Defluorinative Aromatization Reaction of Various β -(ω -Chloroperfluoroalkyl)-*meso*-tetraphenylporphyrins^a



entry	reactant	product	<i>t</i> (min) ^b	yield (%) ^c
1	Zn3b	Zn8	30	98
2	Ni3b	Ni8	30	90
3	Cu3b	Cu8	30	85
4	H₂3b	H₂8	60	60 ^d
5	Zn6b	Zn11	20	95
6	Ni6b	Ni11	20	80
7	Cu6b	Cu11	20	72
8	Zn7b	Zn12	10	40 ^e
9	Ni7b	Ni12	10	20 ^e
10	Cu7b	Cu12	10	8 ^e
11	Zn3a	Zn13	10	98
12	Zn3c	Zn14	10	52 ^f

^a Reactions were carried out in DMSO (10 mL) under N₂ with porphyrin (50 mg, 1.0 equiv) and Na₂S₂O₄/K₂CO₃ (10:10 equiv per R_F tail) at 100 °C. ^b Optimized reaction time. Extended reaction time did not lead to increased yield, and slow degradation of the product was observed. ^c Isolated yields. ^d Intramolecular cyclization product **H₂9** was also obtained in 15% yield. ^e Serious degradation of porphyrins was observed. ^f A significant amount of polar side product porphyrin sulfinate salt was formed.

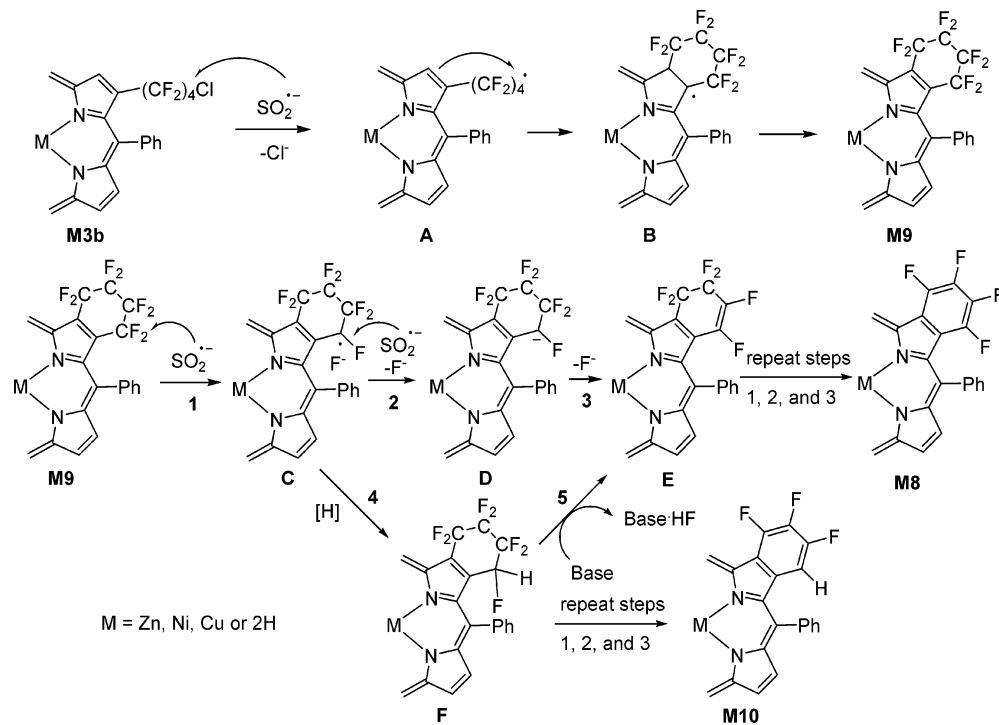
(M = Zn, Ni, or Cu), which partly decompose under strongly reductive conditions. Indeed, the latter electrochemical data point to the fact that the reduction potentials of **Zn12** are lower. Longer reaction time resulted in lower yields of the desired products. In the case of **Zn3a**, the β -perfluoroalkyl porphyrin radical did not attack the adjacent β -position, but the ortho-carbon of the phenyl ring on the adjacent *meso*-position and subsequent reductive defluorinative aromatization provided the fluorinated fused seven-membered porphyrin **Zn13** in quantitative yield (Table 2, entry 11). When using **Zn3c** as a substrate, only H-transfer product **Zn14** was obtained and no intramolecular cyclization aromatization product was observed, which was in line with the reported results (Table 2, entry 12).¹⁷

Mechanism Consideration. On the basis of the above experimental facts and the literature,^{1,2} we propose a possible mechanism for the intramolecular cyclization and reductive defluorinative aromatization reaction. As outlined in Scheme 3, the starting porphyrin **M3b** (M = Zn, Ni, Cu, or 2H), quite similar to R_FI,¹⁶ accepts one electron from the radical anion of sulfur dioxide, produced by decomposition of sodium dithionite, and then dissociates to give radical intermediate **A** and Cl⁻. Radical adds to the β,β' -double bond of the porphyrin to form intermediate **B**, which was easily transformed into intramolecular cyclization product **M9** (M = Zn, Ni, Cu, or 2H). Electron attachment of **M9** (M = Zn, Ni, Cu, or 2H) from the radical anion of sulfur dioxide results in the formation of intermediate **C**, which accepts another electron from the radical anion of sulfur dioxide to provide intermediate **D**, and subsequent fluoride ion elimination leads to the formation of intermediate **E**. An alternative to intermediate **E** is that intermediate **C** abstracts a hydrogen atom to give intermediate **F**, which eliminates a hydrogen fluoride molecule by base to afford intermediate **E**. Repeating steps 1, 2, and 3 of intermediate **E** finally yields the desired products **M8** (M = Zn, Ni, Cu, or 2H).

This possible mechanism reasonably accounts for the fact that a greater amount of Na₂S₂O₄ and stronger base facilitates the formation of the desired products **M8** (M = Zn, Ni, Cu, or 2H). Furthermore, the following experiments support the above proposed mechanism: (1) **Zn9** was isolated and subjected to the reaction under similar conditions, which resulted in the formation of **Zn8** in quantitative yield. (2) When the reaction was carried out with **H₂3b** in the absence of base, a small amount of partial reduction product **H₂10** was indeed isolated, which could be rationally explained by repeating steps 1, 2, and 3 of intermediate **F**. In contrast, no formation of **H₂10** was observed in the presence of base, which might result from the elimination of a hydrogen fluoride molecule of intermediate **F** by the base. (3) When **H₂3b** was used as a substrate at relatively lower temperature (40 °C) for 8 h, partly defluorinated isomers **H₂15** and **H₂16** were obtained in 25% and 5% yield, respectively. By contrast, they were not observed in the absence of base. As is known, the C–Cl bond of perfluoroalkyl chloride cannot be activated under modified sulfinate dehalogenation reaction conditions when the reaction temperature is 40 °C.¹⁵ The formation of **H₂15** and **H₂16** could then be reasonably explained by repeating steps 1, 4, and 5 of **H₂3b** directly (Scheme 4).

X-ray Crystal Structure. ORTEP views of the crystal structures for **Zn8**, **Zn11**, and **Zn12** are shown in Figure 1. Selected bond lengths and bond angles for **Zn11** and **Zn12**

(17) Li, A.; Shtarev, A. B.; Smart, B. E.; Yang, Z. Y.; Luszytk, J.; Ingold, K. U.; Bravo, A.; Dolbier, W. R., Jr. *J. Org. Chem.* **1999**, *64*, 5993–5999.

SCHEME 3. Proposed Mechanism for the Intramolecular Cyclization and Defluorinative Reductive Aromatization of Various β -(ω -chloroperfluoroalkyl)-*meso*-tetraphenylporphyrins


together with previous data for pentacoordinated ZnTPP(H₂O)¹⁸ and Zn8^{6d} are summarized in Table 3.

Coordination around Zn(II) in Zn8, Zn11, and Zn12 is pentacoordinate square pyramidal, a common geometry for Zn(II) porphyrins.¹⁹ The M–N distances are nonequivalent in different tetrafluorobenzoporphyrins because of the existence of tetrafluorobenzo groups. The Zn–N distances of the pyrrolic unit with tetrafluorobenzo groups are longer than those without tetrafluorobenzo groups, which is caused by in-plane elongation of the porphyrin core due to the steric strain and electronic effect enforced by the peripheral substituents.¹⁹ The mechanism of elongation of the porphyrin core is partly explained by repulsion of pyrrolic β – β substituents. Relief of the peripheral steric strain results in, for example, C_{β} – C_{β} > $C_{\beta'}$ – $C_{\beta'}$ and C_{α} – C_m – C_{Ph} > $C_{\alpha'}$ – C_m – C_{Ph} (Table 3). Strong electron-withdrawing substituents on the pyrrolic β -positions will decrease the electron density on its N atom, and the weakened M–N bond will be longer than the other M–N pair. Of the three structure, the difference in the Zn–N distances is larger in Zn11 (0.096 Å) than in Zn8 (0.086 Å), and the Zn–N distances of pyrrolic units with tetrafluorobenzo groups in Zn8, Zn11, and Zn12 are notably longer than those of Zn1, as shown in Table 3.

The magnitude of distortion in the macrocycles of Zn8, Zn11, and Zn12 is demonstrated in Figure 1. An edge-on view of the macrocycle shows clearly that the porphyrin pyrrole rings are alternately tilted up and down with respect to the least-squares plane of the 24 atoms of the porphyrin core, i.e., the macrocycle is distorted into a very nonplanar saddle conformation,^{10,19,20} which presumably minimizes unfavorable contacts between

meso and β substituents. The magnitude of distortion in the macrocycle rises with increasing substitution of tetrafluorobenzo groups to the pyrrole ring, indicated evidently by the fact that average displacements for the pyrrolic β -carbons from the least-squares plane for Zn8, Zn11, and Zn12 are 0.62, 0.93 and 1.31 Å, respectively. Comparison of the root-mean-square of the sum of squares of the deviation of the 24 core atoms from their least-squares plane (Figure 1), also shows clearly the considerable distortion in these complexes, with Zn12 being the most distorted of the three compounds.

UV–Vis Absorption Spectra. In the past, benzoporphyrins have not been easily accessible, and therefore only a few studies of their spectroscopic properties have been accomplished. No doubt, these molecules represent an interesting class of chromophores, and comprehensive photophysical assessment is yet to be done. It is known that red shifts of the ground state spectra may be attributed to some extent to saddling/ruffling of the porphyrin as well as electronic effects due to increased π -conjugation, a notion that is continuously being addressed with a range of substitutions.²¹ A comparative photophysical study as well as some theoretical calculations have been recently published for Zn and Pd complexes of symmetrically extended porphyrins to assess the relative contributions of nonplanar distortion and increased π -conjugation.^{21,14a–e} One of the main conclusions made was that the influence of nonplanar distortion on the red shifts of the optical transitions of laterally extended porphyrins is smaller than that of the π -conjugation. These

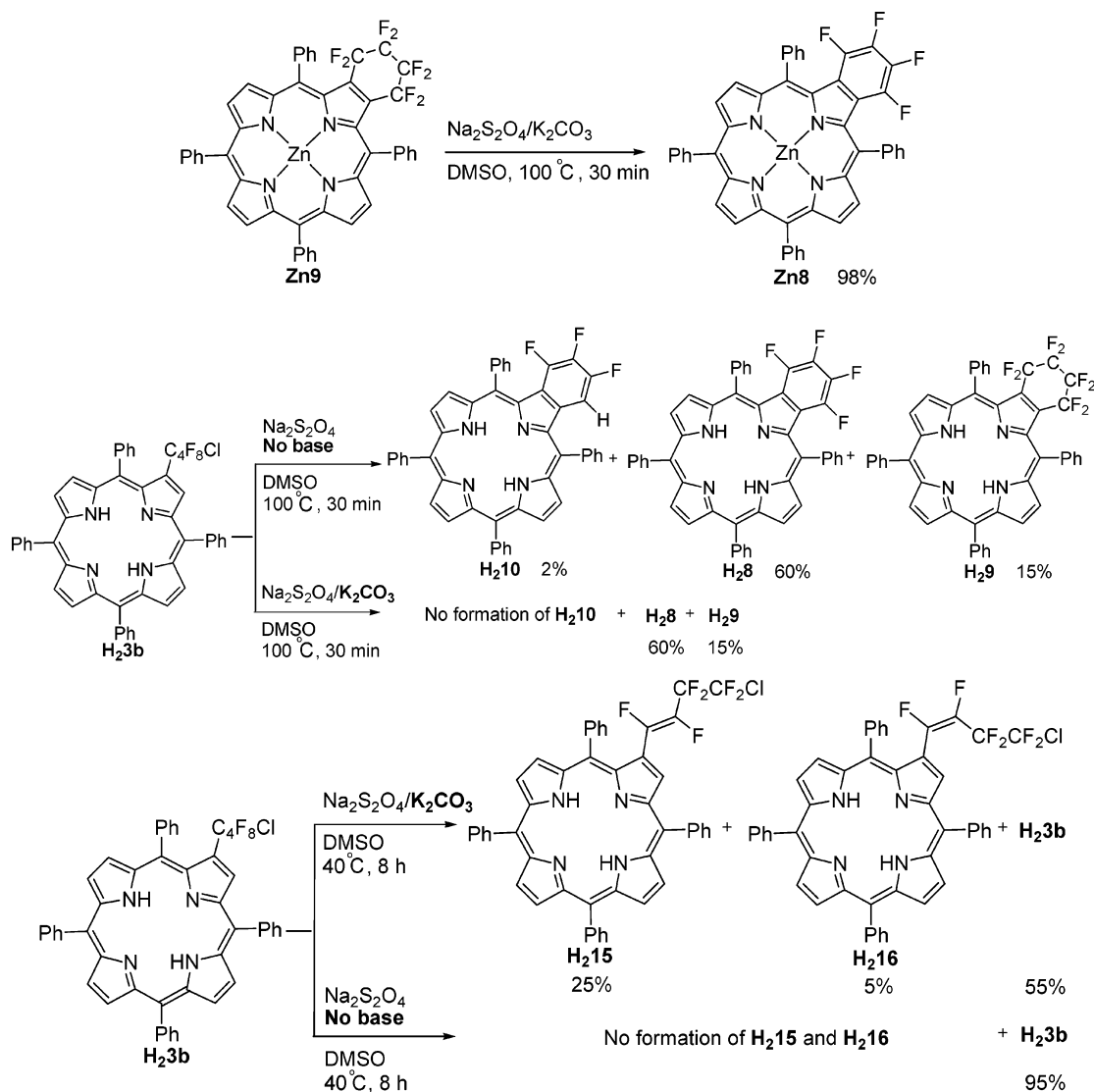
(18) (a) Golder, A. J.; Povey, D. C. *Acta Crystallogr.* **1990**, *C46*, 1210. (b) Terazono, Y.; Patrick, B. O.; Dolphin, D. H. *Inorg. Chem.* **2002**, *41*, 6703–6710.

(19) Scheidt W. R. In *The Porphyrin Handbook*; Kadish, K. M., Smith, K. M., Guillard, R., Eds.; Academic Press: San Diego, CA, 2000; Vol. 3, Chapter 16.

(20) (a) Medforth, C. J.; Senge, M. O.; Smith, K. M.; Sparks, L. D.; Shelnutt, J. A. *J. Am. Chem. Soc.* **1992**, *114*, 9859–9869. (b) Scheidt, W. R.; Lee, Y. J. *Struct. Bonding (Berlin)* **1987**, *64*, 1–70.

(21) For recent and selective reports, see the following: (a) Rogers, J. E.; Nguyen, K. A.; Hufnagle, D. C.; McLean, D. G.; Su, W.; Gossett, K. M.; Burke, A. R.; Vinogradov, S. A.; Pachter, R.; Fleitz, P. A. *J. Phys. Chem. A* **2003**, *107*, 11331–11339. (b) Haddad, R. E.; Gazeau, S.; Pécaut, J.; Marchon, J. C.; Medforth, C. J.; Shelnutt, J. A. *J. Am. Chem. Soc.* **2003**, *125*, 1253–1268.

SCHEME 4. Some Proofs for the Proposed Mechanism



results were mainly based on the analysis of the computationally obtained structures, since few experimental data were available. Herein we present new X-ray data and some additional photophysical measurements, further supporting the above-mentioned conclusion.

As shown in Table 4, compared to the regular *meso*-tetraphenylporphyrin, the tetrafluorobenzoporphyryns exhibit large red shifts of the absorption bands. For example, in the case of **Zn8**, **Zn11**, and **Zn12**, the shifts reach 20, 43, and 97 nm for the Soret bands, respectively. Distortion of the macrocycle of **Zn12** is similar to that of [2,3,7,8,12,13,17,18-octamethyl-5,10,15,20-tetraphenylporphyrinato]zinc (ZnOMTPP) because they have the similar displacement for the pyrrolic β -carbons from the least-squares plane of the porphyrin core (0.93 Å for **Zn12** vs 1.05 Å for ZnOMTPP).^{22a} However, the difference of the Soret band between **Zn12** and **Zn1** reaches 43 nm and that between ZnOMTPP and **Zn1** only 24 nm.^{22b} This implies that the red shift of the absorption bands of laterally extended porphyrins is caused mainly by the extended π -conjugation. In addition, compared with [β -tetra*benzo-meso*-tetraphenylporphyrinato]zinc (ZnTBTPP), **Zn12** is notably bathochromically shifted, and the difference between them reaches up to 61 nm, indicating the large influence of fluorine atoms

(Table 4). These might be ascribed to the fact that the longer C–F bond length (1.4 Å compared to the C–H bond length (1.1 Å)²³ makes the tetrafluorobenzoporphyrin bulkier than the benzo group, which results in increasing macrocycle distortion in **Zn12**, although the van der Waals radius of fluorine is close to that of hydrogen.²⁴

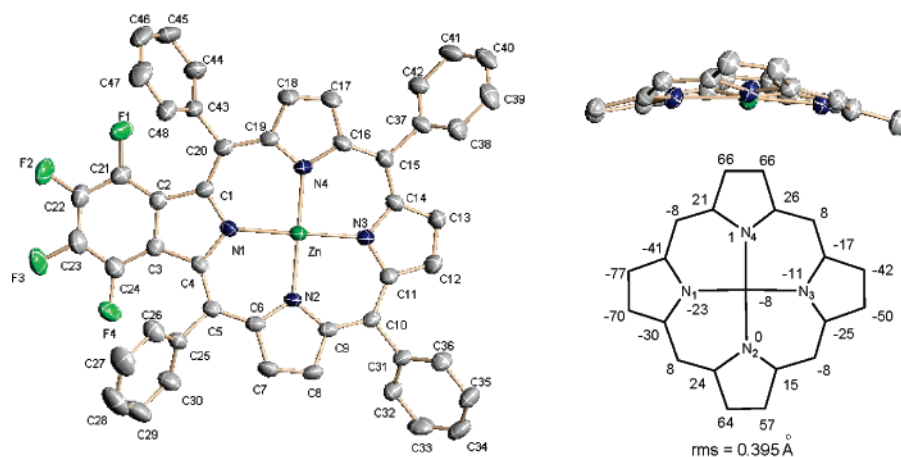
Electrochemistry. The experimental redox potentials for **Zn1**, **Zn8**, **Zn11**, and **Zn12**, determined by cyclic voltammetry, are presented in Table 5. The redox potentials of porphyrins track the energy levels of HOMOs and LUMOs of the complexes, and the differences between the first oxidation and reduction potentials, neglecting solvation effects, provide an indication of the energy of the first absorption band of porphyrins, since this transition is principally a HOMO to LUMO excitation.^{25,26} The electron-withdrawing character of

(22) (a) Barkigia, K. M.; Berber, M. D.; Fajer, J.; Medforth, C. J.; Renner, M. W.; Smith, K. M. *J. Am. Chem. Soc.* **1990**, *112*, 9675. (Erratum to document cited in CA113(24):2234155) (b) Barkigia, K. M.; Berber, M. D.; Fajer, J.; Medforth, C. J.; Renner, M. W.; Smith, K. M. *J. Am. Chem. Soc.* **1990**, *112*, 8851–8857.

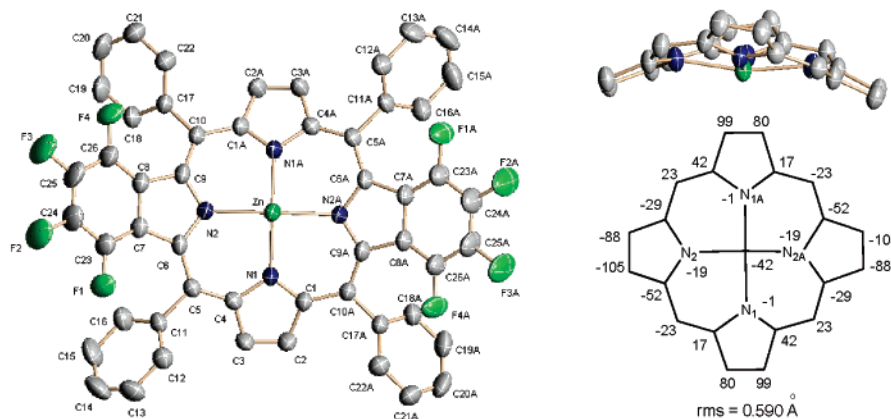
(23) *Handbook of Chemistry & Physics*, 81st ed.; CRC Press: Boca Raton, FL, 2000–2001; pp 9–5.

(24) Cotton, F. A.; Wilkinson, G. *Advanced Inorganic Chemistry*, 3rd ed.; Interscience Publishers: New York, 1972.

a. Zn8



b. Zn11



c. Zn12

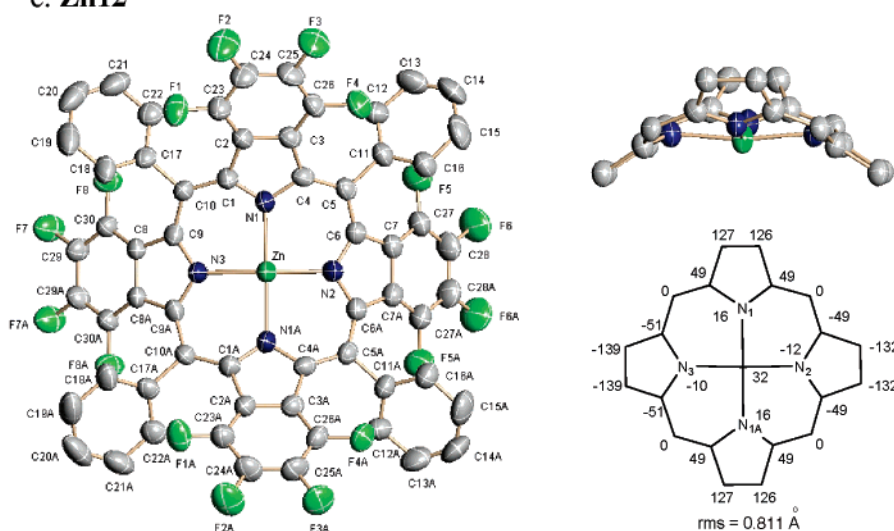
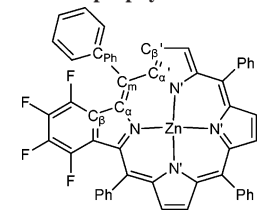


FIGURE 1. X-ray crystal structures (left column) and displacements (in 0.01 Å units) of the porphyrin core atoms from their least-squares plane of the meso carbon atoms (right column) of (a) **Zn8**, (b) **Zn11**, and (c) **Zn12**. The axial ligand, solvated molecules, and hydrogen atoms were omitted for clarity.

the tetrafluorobenzo group is expected to influence significantly the electrochemical properties of the porphyrin derivatives. Consequently, the presence of them at the periphery of the

porphyrin macrocycle stabilizes both the HOMOs and the LUMOs with respect to those of the unsubstituted derivatives. Thus tetrafluorobenzoporphyrins would be easier to reduce and

TABLE 3. Selected Bond Lengths (Å), Angles (deg), and Averages for Various Tetrafluorobenzoporphyrin Zinc Complexes


	Zn8	Zn11	Zn12	Zn1
Zn–N	2.092 (3)	2.106	2.054	
Zn–N'	2.006	2.010		2.050
N–C _α	1.381 (5)	1.361	1.368	
N–C'	1.379	1.371		1.372
C _α –C _β	1.458 (5)	1.456	1.455	
C _α '–C _β '	1.430	1.437		1.442
C _β –C _β	1.401 (5)	1.419	1.413	
C _β '–C _β '	1.337	1.334		1.341
C _α –N–C _α	109.2 (3)	110.1	109.7	
C _α '–N–C _α '	106.1	106.7		106.8
N–C _α –C _β	108.4 (3)	108.4	108.3	
N'–C _α '–C _β '	109.6	109.4		
C _α –C _β –C _β	106.6 (3)	106.1	106.5	
C _α '–C _β '–C _β '	107.1	107.5		
N–C _α –C _m	122.7 (3)	122.4	122.2	
N'–C _α '–C _m	125.0	125.7		
C _α –C _m –C _{Ph}	119.9 (3)	119.5 (3)	118.6	
C _α '–C _m –C _{Ph}	114.2	115.7 (3)		
N1–Zn–N3	175.01 (13)	167.31 (15)	171.6 (2)	
N2–Zn–N4	175.20 (14)	156.05 (16)	155.9 (3)	

TABLE 4. UV–Vis Spectral Data for Various Intramolecular Cyclization Aromatic Porphyrins in CH₂Cl₂ at 25 °C

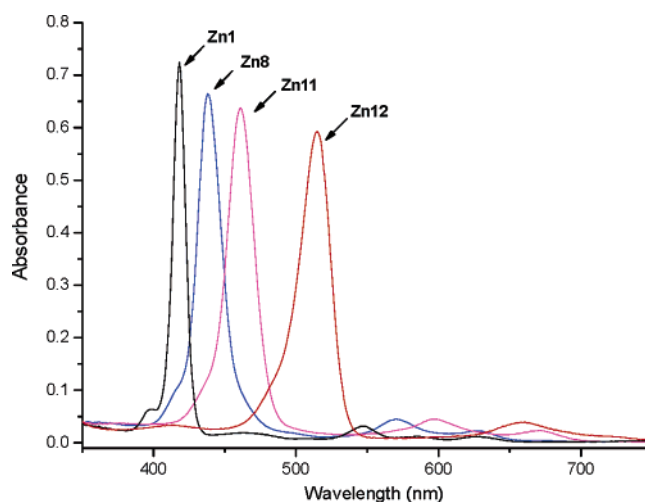
porphyrins	B bands (nm)	Q bands (nm)	
Zn1	418	547	585
Zn8	438	570	629
Zn11	461	599	670
Zn12	515	660	<i>a</i>
ZnTBTPP ^b	454	603	650
Ni1	416	520	<i>a</i>
Ni8	435	551	587
Ni11	452	572	614
Ni12	477	612	660
Cu1	415	538	<i>a</i>
Cu8	434	561	588
Cu11	456	585	628
Cu12	497	623	670

^a Not observed. ^b ZnTBTPP = [β-tetrabenzomeso-tetraphenylporphyrinato]zinc; the data come from ref 10b, p 285.

harder to oxidize. Nevertheless, this is not the case (Table 5). The differences in the reduction potentials $\Delta E_{1/2\text{red(I)}}$ for Zn1/Zn8, Zn8/Zn11, and Zn11/Zn12 range from +0.05 to +0.08 V, while the differences in the oxidation potentials $\Delta E_{1/2\text{ox(I)}}$ for Zn1/Zn8, Zn8/Zn11, and Zn11/Zn12 are negative. These data indicate that the tetrafluorobenzoporphyrins are more readily reduced and oxidized with increasing substitution of

(25) Kadish, K. M.; Caemelbecke, E. V.; Royal G. In *The Porphyrin Handbook*; Kadish, K. M., Smith, K. M., Guillard, R., Eds.; Academic Press: San Diego, CA, 2000; Vol. 8, Chapter 55.

(26) (a) Spyroulias, G. A.; Despotopoulos, A. P.; Raptopoulou, C. P.; Terzis, A.; de Montauzon, D.; Poilblanc, R.; Coutsolelos, A. G. *Inorg. Chem.* **2002**, *41*, 2648–2659. (b) Barkigia, K. M.; Renner, M. W.; Furenlid, L. R.; Medforth, C. J.; Smith, K. M.; Fajer, J. *J. Am. Chem. Soc.* **1993**, *115*, 3627–3635. (c) Ochsenein, P.; Ayougou, K.; Mandon, D.; Fischer, J.; Weiss, R.; Austin, R. N.; Jayaraj, K.; Gold, A.; Ternier, J.; Fajer, J. *Angew. Chem., Int. Ed. Engl.* **1994**, *33*, 348–350.

**FIGURE 2.** UV–vis spectra of various intramolecular cyclization aromatic porphyrin zinc complexes: (black line) Zn1; (blue line) Zn8; (pink line) Zn11; (red line) Zn12.**TABLE 5.** Half-Wave Redox Potentials (V versus SCE) of Various Intramolecular Cyclization Aromatization Porphyrins in CH₂Cl₂ with 0.1 M *n*-Bu₄ClO₄ at 25 °C

por-phyrins	reduction		$\Delta E_{1/2\text{red(I)}}$	oxidation		$\Delta E_{1/2\text{ox(I)}}$	HOMO-LUMO	Soret λ_{max} (nm)
	I	II		I	II			
Zn1	-1.59	<i>a</i>		0.82	1.12		2.41	418
Zn8	-1.51	<i>a</i>	+0.08	0.79	0.98	-0.03	2.30	438
Zn11	-1.44	<i>a</i>	+0.07	0.76	0.90	-0.03	2.22	461
Zn12	-1.39	<i>a</i>	+0.05	0.57	0.77	-0.19	1.98	515

^a Not observed.

tetrafluorobenzoporphyrins. Furthermore, $E_{1/2\text{ox(I)}} - E_{1/2\text{red(I)}}$ decreased with increasing substitution of tetrafluorobenzoporphyrins, indicating decreasing HOMO–LUMO gaps. As a result, the strongly red-shifted Soret and Q absorption bands for them were observed (Table 5).

Redox potentials are governed not only by inductive effect but also by distortion. Electron-withdrawing substituents stabilize the LUMOs and, to a slightly lesser degree, the HOMOs. Macrocyclic distortion destabilizes the HOMOs, leaving the LUMOs relatively unchanged (slight stabilization), and the destabilizing effect on the HOMOs predominates in the severely distorted porphyrins.²⁶ Thus, the negative values of $\Delta E_{1/2\text{ox(I)}}$ for the tetrafluorobenzoporphyrin zinc complexes can be explained if the energy decrease in the HOMOs expected from substitution with additional electron-withdrawing tetrafluorobenzoporphyrins is offset by the macrocycle saddle distortion.

Conclusions

In summary, a convenient and efficient synthesis of various novel fluorinated laterally extended porphyrins has been developed, which is based on the direct intramolecular cyclization and reductive defluorinative aromatization of readily available β-perfluoroalkylated porphyrins by highly selective C–F bond activation under modified sulfinate dehalogenation reaction conditions. This method allows us to readily obtain various potentially valuable tetrafluorobenzoporphyrins in good yields.

It is worth mentioning that further reduction of C–F bonds of the intramolecular cyclization and reductive defluorinative aromatization products are not observed under the optimal conditions, indicating the high selectivity of the reaction. Detailed studies on the reaction conditions and mechanism show that greater amounts of sodium dithionite, stronger base, and Zn(II) central ion of the substrate porphyrins facilitate the formation of the desired intramolecular cyclization and reductive defluorinative aromatization products. Subsequent systematic X-ray crystallographic structure and photophysical and electrochemical properties of a series of novel tetrafluorobenzoporphyrins indicate that the fluorine atoms impose an important influence on the porphyrins. Because of its efficiency and convenience, this method might be useful for some applications in areas such as materials, biomimetics, and medicine. Further studies on the application of this attractive reaction in the synthesis of small molecules with tetrafluorobenzo groups are now in progress.

Experimental Section

Preparation of Free Base β -Mono(ω -chloroperfluoroalkyl)-*meso*-tetraphenylporphyrins. The improved method was adapted from a procedure reported previously for similar porphyrins.^{6d,k} H₂-TPP (**H₂1**) (614 mg, 1.0 mmol) was dissolved in a mixture of DMSO/CH₂Cl₂ (1:2 v/v; 60 mL; solvents were not purified), and then R₁F (**2**) (10 mmol), Na₂S₂O₄ (2.61 g, 15 mmol), and NaHCO₃ (1.26 g, 15 mmol) were added in this order. The mixture was stirred at refluxing for 6–16 h under air, and the course of reaction was monitored by TLC. After cooling to room temperature, the reaction mixture was then directly poured on the top of a column of a short plug of dry silica gel. The column was eluted with CH₂Cl₂. The fractions containing product were collected and washed with water three times. The organic layer was passed through dry silica gel and concentrated to dryness. The resulting residue was purified by dry column chromatography on silica gel (300–400 mesh), using PE/CH₂Cl₂ (3:1 v/v) as eluent. The first dark-purple band was isolated and washed with CH₂Cl₂ to give the desired β -mono(ω -chloroperfluoroalkyl)-*meso*-tetraphenylporphyrins. The products were sufficiently pure to carry through to the next reactions, and an analytical sample was recrystallized from CH₂Cl₂/MeOH.

Porphyrin H₂3a: 25% yield. The spectroscopic data were in agreement with previous work.^{6d}

Porphyrin H₂3b: 30% yield. The spectroscopic data were in agreement with previous work.^{6k}

Porphyrin H₂3c: 35% yield. ¹H NMR (300 MHz, CDCl₃) δ : –2.59 (s, 2H), 7.65–7.83 (m, 12H), 8.13–8.27 (m, 8H), 8.69–8.80 (m, 4H), 8.89–8.93 (m, 2H), 9.07 (s, 1H). ¹⁹F NMR (282 MHz, CDCl₃) δ : –68.27 (m, 2F), –97.58 (m, 2F), –118.23 (s, 2F), –120.46 (s, 2F). MS (ESI) *m/z*: 949.5 (M + H⁺). UV–vis, CH₂Cl₂, λ_{\max} nm (relative intensity): 422 (82.7), 523 (3.7), 555 (1.2), 599 (1.0), 656 (1.8). HRMS (MALDI): calcd for C₅₀H₃₀N₄F₁₂-Cl (M + H⁺) 949.1960, found 949.19619. Anal. Calcd for C₅₀H₃₀N₄F₁₂Cl: C, 63.27; H, 3.08; N, 5.90. Found: C, 63.44; H, 3.46; N, 5.68.

Metalation Reaction of Various Free Base β -Mono(ω -chloroperfluoroalkyl)-*meso*-tetraphenylporphyrins. Zn(II), Ni(II), and Cu(II) were inserted into free base porphyrins according to the procedure reported for similar porphyrins.^{6b,d,e,k} Free base porphyrin **H₂3** (100 mg, 1.0 equiv), M(OAc)₂ (5.0 equiv) (M = Zn, Ni, or Cu), and DMF (10 mL) were heated at refluxing for 1–4 h. The progress of the reaction was monitored by TLC. Upon completion of the reaction, the resulting mixture was cooled to room temperature. There were two workup methods: (1) H₂O (10 mL) was added to the mixture, and the resulting precipitated solid was filtered, washed with water and methanol, and air-dried. (2) The mixture was taken up in CH₂Cl₂, transferred to a separatory funnel,

and washed with water three times. The organic layer was passed through dry silica gel and evaporated to dryness to yield the desired products. This compound was sufficiently pure for further reactions, and an analytical sample was obtained by flash column chromatography (silica gel, 300–400 mesh, PE/CH₂Cl₂ as eluent). Alternatively, Zn(II) could be inserted using CH₂Cl₂/MeOH (4:1 v/v; 10 mL) as solvent at room temperature.

Porphyrin Zn3a: 98% yield. The spectroscopic data were in agreement with previous work.^{6d}

Porphyrin Zn3b: 98% yield. The spectroscopic data were in agreement with previous work.^{6k}

Porphyrin Ni3b: 95% yield. ¹H NMR (300 MHz, CDCl₃) δ : 7.51–7.72 (m, 12H), 7.82–8.00 (m, 8H), 8.59–8.70 (m, 6H), 9.08 (s, 1H). ¹⁹F NMR (282 MHz, CDCl₃) δ : –68.25 (m, 2F), –96.99 (m, 2F), –116.97 (m, 2F), –119.34 (s, 2F). MS (ESI) *m/z*: 905.1 (M + H⁺). UV–vis, CH₂Cl₂, λ_{\max} nm (relative intensity): 421 (41.0), 536 (2.6), 579 (1.0). Anal. Calcd for C₄₈H₂₇N₄F₈CINi·0.5H₂O: C, 63.01; H, 3.08; N, 6.12. Found: C, 63.03; H, 3.37; N, 6.01.

Porphyrin Cu3b: 95% yield. MS (ESI) *m/z*: 910.2 (M + H⁺). UV–vis, CH₂Cl₂, λ_{\max} nm (relative intensity): 419 (62.4), 545 (2.6), 582 (1.0). Anal. Calcd for C₄₈H₂₇N₄F₈ClCu: C, 63.30; H, 2.99; N, 6.15. Found: C, 63.12; H, 3.49; N 5.84.

Porphyrin Zn3c: 98% yield. ¹H NMR (300 MHz, CDCl₃) δ : 7.63–7.85 (m, 12H), 8.11–8.26 (m, 8H), 8.68 (d, *J* = 4.8 Hz, 1H), 8.84 (d, *J* = 4.8 Hz, 1H), 8.94 (d, *J* = 7.8 Hz, 4H), 9.34 (s, 1H). ¹⁹F NMR (282 MHz, CDCl₃) δ : –68.20 (m, 2F), –96.65 (m, 2F), –117.58 (s, 2F), –120.37 (s, 2F), –121.52 (m, 4F). MS (MALDI) *m/z*: 1010.1 (M⁺). UV–vis, CH₂Cl₂, λ_{\max} nm (relative intensity): 423 (57.7), 554 (2.2), 595 (1.0). HRMS (MALDI): calcd for C₅₀H₂₇N₄F₁₂ClZn (M⁺) 1010.1022, found 1010.10186. Anal. Calcd for C₅₀H₃₀N₄F₁₂Cl: C, 63.27; H, 3.08; N, 5.90. Found: C, 63.44; H, 3.46; N, 5.68.

General Procedure for Preparation of β -Di- and β -Tetra(ω -chloroperfluorobutyl)-*meso*-tetraphenylporphyrin Metal Complexes. The method was adapted from a procedure previously reported for similar porphyrins,^{6f} but no poisonous AsPh₃ ligand was used.

Porphyrin Cu6b: 82% yield. Bromoporphyrin **Cu4** (100 mg, 0.1 mmol, 1.0 equiv), Pd₂(dba)₃·CHCl₃ (10 mg, 10 mol %), and Cu (128 mg, 20 equiv) (Note: Copper powder used was synthesized by the reduction reaction of CuSO₄·5H₂O with Zn.^{6b}) were added to a Schlenk flask (50 mL). The flask was then evacuated and backfilled with nitrogen (three cycles). DMSO (20 mL) and IC₄F₈-Cl (**2b**) (363 mg, 10 equiv) were charged with a syringe at room temperature. The reaction mixture was stirred at 100 °C for 4 h and then allowed to reach room temperature. The reaction mixture was diluted with CH₂Cl₂ (20 mL) and filtered through a short plug of dry silica gel. The solvent was washed three times with water. The organic layer was passed through dry silica gel and evaporated to dryness. The resulting solid was purified by flash chromatography (silica gel, 300–400 mesh, PE as eluent) to yield the desired **Cu6b**. MS (MALDI) *m/z*: 1143.0 (M⁺). UV–vis, CH₂Cl₂, λ_{\max} nm (relative intensity): 424 (30.4), 553 (1.0), 593 (1.0). Anal. Calcd for C₅₂H₂₆N₄F₁₆Cl₂Cu: C, 54.54; H, 2.29; N, 4.89. Found: C, 54.30; H, 2.21; N, 5.01.

Porphyrin Ni6b: 85% yield. This was prepared as described above for **Cu6b**. Bromoporphyrin **Ni4** (100 mg, 0.1 mmol, 1.0 equiv), Pd₂(dba)₃·CHCl₃ (10 mg, 10 mol %), IC₄F₈-Cl (**2b**) (363 mg, 10 equiv), and Cu (128 mg, 20 equiv) were used, and the reaction resulted in the desired **Ni6b** in good yield. ¹⁹F NMR (282 MHz, CDCl₃) δ : –68.21 (m, 4F), –98.23 (m, 4F), –117.44 (m, 4F), –119.57 (m, 4F). MS (MALDI) *m/z*: 1138.1 (M⁺). UV–vis, CH₂Cl₂, λ_{\max} nm (relative intensity): 428 (19.5), 547 (1.0), 588 (1.0). Anal. Calcd for C₅₂H₂₆N₄F₁₆Cl₂Ni·H₂O: C, 53.92; H, 2.44; N, 4.84. Found: C, 54.13; H, 2.38; N, 4.77.

Porphyrin Zn6b: 95% yield for two steps. This was prepared by two steps: (1) Demetallation of **Cu6b** gave free base porphyrin **H₂6b**. (2) Zn(II) was inserted into **H₂6b** to provide the desired

Zn6b. Cu6b (100 mg, 0.0875 mmol) was dissolved in CF_3COOH /concentrated H_2SO_4 (4:1 v/v, 5 mL) and CH_2Cl_2 (5 mL). The mixture was stirred at room temperature for 2 h, then poured carefully into ice water, and extracted with CH_2Cl_2 (15 mL). The organic layer was washed with saturated NaHCO_3 solution once and water twice. Then $\text{Zn}(\text{OAc})_2 \cdot 4\text{H}_2\text{O}$ (96 mg, 5.0 equiv) and MeOH (5 mL) were added to the solution, and the resulting mixture was stirred for 1 h at room temperature. The mixture was washed with water three times, passed through dry silica gel, and evaporated to dryness to yield the desired **Zn6b**. This compound was sufficiently pure for further reactions, and an analytical sample was obtained by flash column chromatography (silica gel, 300–400 mesh, $\text{PE}/\text{CH}_2\text{Cl}_2$ as eluent). ^{19}F NMR (282 MHz, CDCl_3) δ : -68.79 (s, 4F), -97.17 (m, 4F), -117.46 (m, 4F), -119.81 (m, 4F). MS (MALDI) m/z : 1144.0 (M^+). UV-vis, CH_2Cl_2 , λ_{max} nm (relative intensity): 427 (29.6), 561 (1.0), 604 (1.1). Anal. Calcd for $\text{C}_{52}\text{H}_{26}\text{N}_4\text{F}_{16}\text{Cl}_2\text{Zn} \cdot \text{H}_2\text{O}$: C, 53.61; H, 2.42; N, 4.81. Found: C, 53.65; H, 2.10; N, 4.65.

Porphyrin Cu7b: 75% yield. According to the procedure given for the preparation of **Cu6b**, bromoporphyrin **Cu5** (100 mg, 0.0765 mmol, 1.0 equiv), $\text{Pd}_2(\text{dba})_3 \cdot \text{CHCl}_3$ (8 mg, 10 mol %), $\text{ICl}_4\text{F}_8\text{Cl}$ (**2b**) (555 mg, 20 equiv), and Cu (196 mg, 40 equiv) were used, and the reaction was carried out for 1 h, resulting in the desired **Cu7b** in good yield. MS (MALDI) m/z : 1611.0 (M^+). UV-vis, CH_2Cl_2 , λ_{max} nm (relative intensity): 439 (16.6), 582 (1.0), 630 (1.1). Anal. Calcd for $\text{C}_{60}\text{H}_{24}\text{N}_4\text{F}_{32}\text{Cl}_4\text{Cu}$: C, 44.64; H, 1.50; N, 3.47. Found: C, 44.40; H, 1.61; N, 3.38.

Porphyrin Ni7b: 80% yield. Similar to the procedure given for **Cu6b**, bromoporphyrin **Ni5** (100 mg, 0.0768 mmol), $\text{Pd}_2(\text{dba})_3 \cdot \text{CHCl}_3$ (8 mg, 10 mol %), $\text{ICl}_4\text{F}_8\text{Cl}$ (**2b**) (555 mg, 20 equiv), and Cu (196 mg, 40 equiv) were used, and the reaction resulted in the desired **Ni7b** in good yield. MS (MALDI) m/z : 1606.0 (M^+). UV-vis, CH_2Cl_2 , λ_{max} nm (relative intensity): 443 (30.7), 559 (1.9), 603 (1.0). Anal. Calcd for $\text{C}_{60}\text{H}_{24}\text{N}_4\text{F}_{32}\text{Cl}_4\text{Ni}$: C, 44.78; H, 1.50; N, 3.48. Found: C, 44.89; H, 1.75; N, 3.32.

Porphyrin Zn7b: 95% yield for the two steps. Using the procedure described for **Zn6b**, **Cu7b** (100 mg, 0.062 mmol) was used, and the reactions afforded the desired **Zn7b** in excellent yield. MS (MALDI) m/z : 1612.0 (M^+). UV-vis, CH_2Cl_2 , λ_{max} nm (relative intensity): 453 (25.4), 601 (1.0), 655 (1.6). Anal. Calcd for $\text{C}_{60}\text{H}_{24}\text{N}_4\text{F}_{32}\text{Cl}_4\text{Zn} \cdot \text{MeOH}$: C, 44.46; H, 1.71; N, 3.40. Found: C, 44.58; H, 1.73; N, 2.91.

General Procedure for Intramolecular Cyclization and Reductive Defluorinative Aromatization of Various β -(ω -Chloroperfluoroalkyl)-meso-tetraphenylporphyrins. β -(ω -Chloroperfluoroalkyl)-meso-tetraphenylporphyrin (50 mg, 1.0 equiv) was dissolved in DMSO (20 mL) and heated to 100 °C, and then $\text{Na}_2\text{S}_2\text{O}_4$ (10 equiv) and K_2CO_3 (10 equiv) were added. The mixture was stirred under nitrogen for 10–30 min and cooled to room temperature, and CH_2Cl_2 (20 mL) was added. The mixture was then washed with water three times. The organic layer was passed through dry silica gel and evaporated to dryness. The resulting solid was purified by flash column chromatography (silica gel, 300–400 mesh, $\text{PE}/\text{CH}_2\text{Cl}_2$ or PE/THF as eluent) to yield the desired products in good yields.

Porphyrin Zn8: 98% yield. The spectroscopic data were in agreement with previous work.^{6d}

Porphyrin Zn9: This porphyrin was isolated as side product. The spectroscopic data were in agreement with previous work.^{6d}

Porphyrin Ni8: 90% yield. ^1H NMR (300 MHz, CDCl_3) δ : 7.69 (d, 12H), 8.00–8.23 (m, 8H), 8.52–8.60 (m, 6H). ^{19}F NMR (282 MHz, CDCl_3) δ : -130.35 (d, $J = 19.2$ Hz, 2F), -157.05 (d, $J = 18.6$ Hz, 2F). MS (MALDI) m/z : 792.2 (M^+). UV-vis, CH_2Cl_2 , λ_{max} nm (relative intensity): 435 (26.0), 551 (1.8), 587 (1.0). Anal. Calcd for $\text{C}_{48}\text{H}_{26}\text{N}_4\text{F}_4\text{Ni} \cdot 2\text{EtOH}$: C, 70.69; H, 4.11; N, 6.34. Found: C, 70.71; H, 4.16; N, 6.34.

Porphyrin Cu8: 82% yield. MS (MALDI) m/z : 797.1 (M^+). UV-vis, CH_2Cl_2 , λ_{max} nm (relative intensity): 434 (38.5), 561 (2.5), 588 (1.0). HRMS (MALDI): calcd for $\text{C}_{48}\text{H}_{26}\text{N}_4\text{F}_4\text{Cu}$ (M^+)

797.1380, found 797.13841. Anal. Calcd for $\text{C}_{48}\text{H}_{26}\text{N}_4\text{F}_4\text{Cu} \cdot 2\text{EtOH}$: C, 70.30; H, 4.08; N, 6.31. Found: C, 70.61; H, 4.10; N, 5.98.

Porphyrin H28: 60% yield. The spectroscopic data were in agreement with previous work.^{6d}

Porphyrin H29: 15% yield. The spectroscopic data were in agreement with previous work.^{6d}

Porphyrin H210: 2% yield. No base was used. ^1H NMR (300 MHz, CDCl_3) δ : -2.60 (s, 2H), 6.64–6.69 (m, 1H), 7.79–7.97 (m, 12H), 8.22–8.30 (m, 8H), 8.68 (s, 2H), 8.82–8.86 (m, 4H). ^{19}F NMR (282 MHz, CDCl_3) δ : -126.14 (m, 1F), -134.43 (m, 1F), -161.78 (m, 1F). MS (MALDI) m/z : 719.4 ($\text{M} + \text{H}^+$). UV-vis, CH_2Cl_2 , λ_{max} nm (relative intensity): 429 (45.9), 478 (2.6), 523 (2.5), 601 (1.0). HRMS (MALDI): calcd for $\text{C}_{48}\text{H}_{30}\text{N}_4\text{F}_3$ ($\text{M} + \text{H}^+$) 719.2388, found 719.24171.

Porphyrin Zn11: 95% yield. ^1H NMR (300 MHz, CDCl_3) δ : 7.76–7.80 (m, 12H), 8.23–8.26 (m, 8H), 8.55 (s, 4H). ^{19}F NMR (282 MHz, CDCl_3) δ : -130.57 (d, $J = 19.2$ Hz, 4F), -156.49 (d, $J = 18.9$ Hz, 4F); MS (MALDI) m/z : 920.1 (M^+). UV-vis, CH_2Cl_2 , λ_{max} nm (relative intensity): 461 (27.2), 599 (1.9), 670 (1.0). Anal. Calcd for $\text{C}_{52}\text{H}_{24}\text{N}_4\text{F}_8\text{Zn} \cdot 2\text{H}_2\text{O}$: C, 65.18; H, 2.95; N, 5.85. Found: C, 65.52; H, 2.62; N, 5.36.

Porphyrin Ni11: 80% yield. The spectroscopic data were in agreement with previous work.^{6f}

Porphyrin Cu11: 72% yield. MS (MALDI) m/z : 919.1 (M^+). UV-vis, CH_2Cl_2 , λ_{max} nm (relative intensity): 456 (29.7), 585 (2.9), 628 (1.0). Anal. Calcd for $\text{C}_{52}\text{H}_{24}\text{N}_4\text{F}_8\text{Cu} \cdot 1.5\text{H}_2\text{O}$: C, 65.93; H, 2.87; N, 5.91. Found: C, 65.86; H, 2.38; N, 5.41.

Porphyrin Zn12: 40% yield. ^1H NMR (300 MHz, CDCl_3) δ : 7.81 (br s, 12H), 8.33 (br s, 8H). ^{19}F NMR (282 MHz, CDCl_3) δ : -131.07 (d, $J = 14.1$ Hz, 8F), -157.77 (d, $J = 14.1$ Hz, 8F). MS (MALDI) m/z : 1164.1 (M^+). UV-vis, CH_2Cl_2 , λ_{max} nm (relative intensity): 413 (1.0), 515 (17.6), 660 (1.2). HRMS (MALDI) calcd for $\text{C}_{60}\text{H}_{20}\text{N}_4\text{F}_{16}\text{Zn}$ (M^+) 1164.0719, found 1164.07184. Anal. Calcd for $\text{C}_{60}\text{H}_{20}\text{N}_4\text{F}_{16}\text{Zn} \cdot 1.5\text{THF}$: C, 62.20; H, 2.53; N, 4.55. Found: C, 62.87; H, 2.14; N, 4.55.

Porphyrin Ni12: 20% yield. ^1H NMR (300 MHz, CDCl_3) δ : 7.72 (br s, 12H), 7.96–7.98 (m, 8H). ^{19}F NMR (282 MHz, CDCl_3) δ : -129.42 (d, $J = 16.1$ Hz, 8F), -155.31 (d, $J = 14.9$ Hz, 8F). MS (MALDI) m/z : 1158.1 (M^+). UV-vis, CH_2Cl_2 , λ_{max} nm (relative intensity): 477 (17.7), 612 (1.0), 660 (3.4). HRMS (MALDI): calcd for $\text{C}_{60}\text{H}_{20}\text{N}_4\text{F}_{16}\text{Ni}$ (M^+) 1158.07774, found 1158.07804. Anal. Calcd for $\text{C}_{60}\text{H}_{20}\text{N}_4\text{F}_{16}\text{Ni} \cdot 0.5\text{THF}$: C, 62.29; H, 2.02; N, 4.69. Found: C, 62.50; H, 2.01; N, 4.23.

Porphyrin Cu12: 8% yield. MS (MALDI) m/z : 1163.1 (M^+). UV-vis, CH_2Cl_2 , λ_{max} nm (relative intensity): 413 (2.0), 497 (17.8), 623 (1.0), 670 (1.3). Anal. Calcd for $\text{C}_{60}\text{H}_{20}\text{N}_4\text{F}_{16}\text{Cu} \cdot 2\text{THF}$: C, 62.41; H, 2.77; N, 4.28. Found: C, 62.40; H, 2.97; N, 3.92.

Porphyrin Zn13: 98% yield. The spectroscopic data were in agreement with previous work.^{6d}

Porphyrin Zn14: 52% yield. ^1H NMR (300 MHz, CDCl_3) δ : 6.02 (tt, $J_1 = 52.2$ Hz, $J_2 = 5.4$ Hz, 1H), 7.59–7.81 (m, 12H), 8.08–8.22 (m, 8H), 8.64 (d, $J = 4.8$ Hz, 1H), 8.80 (d, $J = 4.8$ Hz, 1H), 8.90 (d, $J = 5.4$ Hz, 4H), 9.31 (s, 1H). ^{19}F NMR (282 MHz, CDCl_3) δ : -96.59 (m, 2F), -117.66 (s, 2F), -121.56 (s, 2F), -123.96 (s, 2F), -130.09 (m, 2F), -137.44 (m, 2F). MS (MALDI) m/z : 976.1 (M^+). UV-vis, CH_2Cl_2 , λ_{max} nm (relative intensity): 423 (58.8), 553 (2.3), 594 (1.0). Anal. Calcd for $\text{C}_{50}\text{H}_{28}\text{N}_4\text{F}_2\text{Zn}$: C, 61.39; H, 2.89; N, 5.73. Found: C, 61.70; H, 3.34; N, 5.39.

Reductive Defluorination Reaction of Free Base Porphyrin H23c. A mixture of **H23c** (100 mg, 0.118 mmol, 1.0 equiv), $\text{Na}_2\text{S}_2\text{O}_4$ (205 mg, 10 equiv), and K_2CO_3 (163 mg, 10 equiv) was stirred in DMSO (20 mL) under nitrogen at 40 °C for 8 h. After cooling to room temperature, the reaction mixture was diluted with CH_2Cl_2 (20 mL) and washed with water three times. The organic layer was passed through dry silica gel and evaporated to dryness. The resulting solid was purified by dry column chromatography (silica gel, 300–400 mesh, $\text{PE}/\text{CH}_2\text{Cl}_2$, 4:1 v/v). The two dark-purple

bands were isolated and washed with CH₂Cl₂. The first band was **H₂16** and second **H₂15**.

Porphyrin H₂15: 25% yield. ¹H NMR (300 MHz, CDCl₃) δ: -2.67 (s, 2H), 7.69–7.86 (m, 12H), 8.21–8.28 (m, 8H), 8.78 (s, 2H), 8.88–8.98 (m, 5H). ¹⁹F NMR (282 MHz, CDCl₃) δ: -71.63 (s, 2F), -114.14 (dt, *J*₁ = 146 Hz, *J*₂ = 23.7 Hz, 1F), -115.11 (m, 2F), -160.83 (d, *J* = 143 Hz, 1F). MS (MALDI) *m/z*: 811.2 (M + H⁺). UV–vis, CH₂Cl₂, λ_{max} nm (relative intensity): 423 (78.5), 520 (3.2), 557 (1.0), 597 (1.0), 654 (1.7). Anal. Calcd for C₄₈H₂₉N₄F₆Cl: C, 71.07; H, 3.60; N, 6.91; F, 14.05. Found: C, 70.71; H, 3.71; N, 6.47; F, 14.05.

Porphyrin H₂16: 5% yield. ¹H NMR (300 MHz, CDCl₃) δ: -2.72 (s, 2H), 7.77–7.80 (m, 12H), 8.21–8.23 (m, 8H), 8.78–8.99 (m, 7H). ¹⁹F NMR (282 MHz, CDCl₃) δ: -70.17 (m, 2F), -88.44 (m, 1F), -114.19 (m, 2F), -149.70 (m, 1F). MS (ESI) *m/z*: 811.2 (M + H⁺). UV–vis, CH₂Cl₂, λ_{max} nm (relative intensity): 422 (77.1), 520 (2.5), 554 (1.3), 596 (1.0), 652 (1.4).

HRMS (ESI): calcd for C₄₈H₃₀N₄F₆Cl (M + H⁺) 811.2049710, found 811.2057703.

Acknowledgment. Financial support from the Natural Science Foundation of China (Nos. 20272026, D20032010, and 20532040) is gratefully acknowledged. We also thank Assistant Professor Jie Sun for resolution of X-ray crystallography and Dr. Xiao-Hua Li of East China Normal University for obtaining electrochemical data.

Supporting Information Available: General methods, CIF files for **Zn11** and **Zn12**, and copies of typical ¹H and ¹⁹F NMR spectra of porphyrins **Zn3a**, **Zn3b**, **Zn3c**, **Zn8**, **Zn9**, **H₂8**, **H₂9**, **H₂10**, **Zn11**, **Zn12**, **Zn13**, **Zn14**, **H₂15**, and **H₂16**. This material is available free of charge via the Internet at <http://pubs.acs.org>.

JO061743R